A systematic study of light dependency of persistent photoconductivity in a-InGaZnO thin-film transistors

Yalan Wang(王雅兰), Mingxiang Wang(王明湘), Dongli Zhang(张冬利), Huaisheng Wang(王槐生)

Citation: Chin. Phys. B . 2020, 29(11): 118101 . **doi:** 10.1088/1674-1056/abb222
Journal homepage: http://cpb.iphy.ac.cn; http://iopscience.iop.org/cpb

What follows is a list of articles you may be interested in

Mg acceptor activation mechanism and hole transport characteristics in highly Mg-doped AlGaN alloys

Qing-Jun Xu(徐庆君), Shi-Ying Zhang(张士英), Bin Liu(刘斌), Zhen-Hua Li(李振华), Tao Tao(陶涛), Zi-Li Xie(谢自力), Xiang-Qian Xiu(修向前), Dun-Jun Chen(陈敦军), Peng Chen(陈鹏), Ping Han(韩平), Ke Wang(王科), Rong Zhang(张荣), You-Liao Zheng(郑有炓)

Chin. Phys. B . 2020, 29(5): 058103 . **doi:** 10.1088/1674-1056/ab7e93

Characteristics of AlGaN/GaN high electron mobility transistors on metallic substrate

Minglong Zhao(赵明龙), Xiansheng Tang(唐先胜), Wenxue Huo(霍雯雪), Lili Han(韩丽丽), Zhen Deng(邓震), Yang Jiang(江洋), Wenxin Wang(王文新), Hong Chen(陈弘), Chunhua Du(杜春花), Haiqiang Jia(贾海强)

Chin. Phys. B . 2020, 29(4): 048104 . **doi:** 10.1088/1674-1056/ab7d9c

Comparison study of GaN films grown on porous andplanar GaN templates

Shan Ding(丁姗), Yue-Wen Li(李悦文), Xiang-Qian Xiu(修向前), Xue-Mei Hua(华雪梅), Zi-Li Xie(谢自力), Tao Tao(陶涛), Peng Chen(陈鹏), Bin Liu(刘斌), Rong Zhang(张荣), You-Dou Zheng(郑有炓)

Chin. Phys. B . 2020, 29(3): 038103 . **doi:** 10.1088/1674-1056/ab6c48

Positive gate bias stress-induced hump-effect in elevated-metal metal-oxide thin film transistors

Dong-Yu Qi(齐栋宇), Dong-Li Zhang(张冬利), Ming-Xiang Wang(王明湘)

Chin. Phys. B . 2017, 26(12): 128101 . **doi:** 10.1088/1674-1056/26/12/128101

Tunable structural color of anodic tantalum oxide films

Sheng Cui-Cui, Cai Yun-Yu, Dai En-Mei, Liang Chang-Hao

Chin. Phys. B . 2012, 21(8): 088101 . **doi:** 10.1088/1674-1056/21/8/088101

A systematic study of light dependency of persistent photoconductivity in a-InGaZnO thin-film transistors*

Yalan Wang(王雅兰), Mingxiang Wang(王明湘)†, Dongli Zhang(张冬利)‡, and Huaisheng Wang(王槐生)

School of Electronic and Information Engineering, Soochow University, Suzhou 215006, *China*

(Received 9 July 2020; revised manuscript received 18 August 2020; accepted manuscript online 25 August 2020)

Persistent photoconductivity (PPC) effect and its light-intensity dependence of both enhancement and depletion (E-/D-) mode amorphous InGaZnO (a-IGZO) thin-film transistors (TFTs) are systematically investigated. Density of oxygen vacancy (V_O) defects of E-mode TFTs is relatively small, in which formation of the photo-induced metastable defects is thermally activated, and the activation energy (E_a) decreases continuously with increasing light-intensity. Density of V_O defects of D-mode TFTs is much larger, in which the formation of photo-induced metastable defects is found to be spontaneous instead of thermally activated. Furthermore, for the first time it is found that a threshold dose of light-exposure is required to form fully developed photo-induced metastable defects. Under low light-exposure below the threshold, only a low PPC barrier is formed and the PPC recovery is fast. With increasing the light-exposure to the threshold, the lattice relaxation of metal cations adjacent to the doubly ionized oxygen vacancies (V_O^{2+}) is fully developed, and the PPC barrier increases to ~ 0.25 eV, which remains basically unchanged under higher light-exposure. Based on the density of V_O defects in the channel and the condition of light illumination, a unified model of formation of photo-induced metastable defects in a-IGZO TFTs is proposed to explain the experimental observations.

Keywords: amorphous indium-gallium-zinc oxide, thin-film transistors, persistent photoconductivity, light-intensity

PACS: 81.05.Gc, 81.05.Ea, 85.30.Tv **DOI:** 10.1088/1674-1056/abb222

1. Introduction

Transparent amorphous oxide semiconductors represented by amorphous InGaZnO (a-IGZO) thin-film transistors (TFTs) have attracted much attention. Compared to hydrogenated amorphous silicon (a-Si:H) TFTs, they have higher field effect mobility, lower subthreshold swing, wider band gap ($\sim$ 3.2 eV), and optical transparency.[1,2] It is known that a-IGZO TFTs have persistent photoconductivity (PPC) effect,[3,4] i.e, their photoconductivity lasts for a long period of time after the illumination is stopped. It has potential applications such as bistatic optical switches,[5] radiation detectors,[6] and photoelectric memories.[7] It is generally believed that the PPC effect of metal oxide semiconductors is related to doubly ionized oxygen vacancies (V_O^{2+}) metastable defects, which are generated by ionization of neutral V_O induced by photo-excitation.[3,4] They are metastable because the neighboring metal cations undergo outward lattice relaxation and form a potential barrier which hinders the recombination of electrons and V_O^{2+}.[8,9]

Previous studies have reported light-intensity dependence of PPC effect. Kim *et al.* observed that PPC recovery slowed down with increasing the light-intensity in a-IGZO TFTs,[10] while Lu *et al.* observed the opposite dependency in ZnO films.[7,11,12] In other semiconductor materials,[13–15] Singh *et al.* observed that PPC recovery slowed down with increasing the light-intensity in Se–Ge–In related materials,[13] while Polyakov *et al.* reported an opposite dependency in AlGaN[14] and GaN.[15] It is noted that there are no reasonable explanations for these contradictory observations, and a systematic study is needed.

In a-IGZO TFTs, the V_O defect in the channel layer is critical to TFT characteristics. It can be adjusted by changing the thickness of the active layer[16] or cover layer[17] and thermal annealing conditions.[18,19] Correspondingly, the turn-on voltage (V_{ON}) from the off-state to the subthreshold region of a TFT can be adjusted to realize enhancement/depletion (E-/D-) mode. In this study, we choose both kinds of a-IGZO TFTs, which have large different V_O defects, to systematically study the light dependence of the PPC effect. The density of V_O defects in E-mode TFTs is relatively small, in which the formation of the photo-induced metastable defects is thermally activated. The density of V_O defects in D-mode TFTs is much larger, in which the formation of photo-induced metastable defects is found to be spontaneous. Furthermore, for the first time it is found that a threshold dose of light-exposure is required to form fully developed photo-induced metastable de-

*Project supported in part by the National Natural Science Foundation of China (Grant Nos. 61974101 and 61971299), the State Key Laboratory of ASIC and System, Fudan University (Grant No. 2019KF007), the Natural Science Foundation of Jiangsu Province, China (Grant No. SBK2020021406), the Natural Science Foundation of the Jiangsu Higher Education Institutions of China (Grant No. 19KJB510058), and the Suzhou Science and Technology Bureau (Grant No. SYG201933).

†Corresponding author. E-mail: mingxiang_wang@suda.edu.cn

‡Corresponding author. E-mail: dongli_zhang@suda.edu.cn

fects. Based on the density of V_O defects in the channel and the condition of light illumination, a unified model of formation of photo-induced metastable defects in a-IGZO TFTs is proposed.

2. Experiments

Inverted staggered bottom gate a-IGZO TFTs are used as shown in Fig. 1. For E-mode TFTs, a 100 nm thick Mo gate electrode was sputtered, and 120 nm gate oxide layer was deposited by plasma-enhanced chemical vapor deposition (PECVD) at 300 °C. Then, 50 nm thick a-IGZO channel layer was deposited by RF magnetron sputtering at room temperature. A 50 nm thick PECVD SiO_2 was used as the etching stop layer (ESL). Contact holes were opened by dry etching and source/drain (S/D) electrodes were sputtered. Finally, 100 nm SiO_2 passivation layer was deposited. TFTs were annealed at 300 °C for 1 h in the air. Device channel width (W) and length (L) are 10 μm and 5 μm, respectively. For D-mode TFTs, the fabrication process is similar, while the ESL (100 nm) and passivation layer (250 nm) are thicker, and W/L are 10 μm/20 μm.

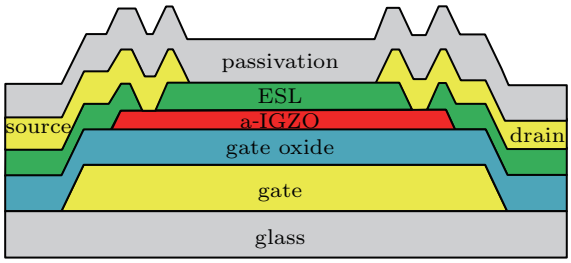

Fig. 1. Schematic cross-sectional diagram of an inverted staggered back gate a-IGZO TFT.

Transfer characteristic curves and sampling of drain current (I_D) were measured by Agilent 4156C semiconductor parameter analyzer. Transfer curves of $V_{DS} = 1$ V were measured in dark or under red/green/blue/UV light illumination. LED monochromatic light-sources were used, including red 660 nm (1.88 eV), green 520 nm (2.38 eV), blue 445 nm (2.79 eV), and UV 395 nm (3.14 eV) ones. PPC effect was investigated with blue light illumination. I_D photo-response and recovery were sampled at $V_{DS} = 1$ V and $V_{GS} = V_{ON}$, and the sampling time interval is 1 s.

3. Results and discussion

3.1. TFTs photo-responses

Figure 2 shows the transfer curves of the two kinds of TFTs in both logarithmic and linear scales, measured in dark or under illumination with a chosen wavelength light-intensity at 1 mW/cm^2. In dark, V_{ON} of E-/D-mode a-IGZO TFTs are 3.0 V/−12 V, respectively. Under red light, both TFTs have no photo-response, and the transfer curves in both logarithmic and linear scales coincide with those in the dark. Under green light, the E-mode TFT has a slight photo-response, with its transfer curve at V_{ON} negatively shifted by −0.2 V, while the D-mode TFT has an obvious photo-response with a larger negative shift of −0.5 V at V_{ON}. Under blue and UV lights, the photo-response of both TFTs is significant. There are large negative shifts in V_{ON} and the threshold voltage (V_{th}), as well as a significant increase in I_D. Besides, the photo-response of the D-mode TFT is much more sensitive than the E-mode one. Such photo-response can be well understood with neutral V_O ionization model.[8,9] The photon energy of red light, 1.9 eV, is much lower than the required ionization energy of V_O defects,[8,9,20] while that of green light, 2.38 eV, should be slightly higher than it, which is ∼2.3 eV as reported in literatures.[8,9,20] The D-mode TFT is more responsive, implying that its V_O defects density is higher and/or its DOS trap levels in the band-gap are higher.

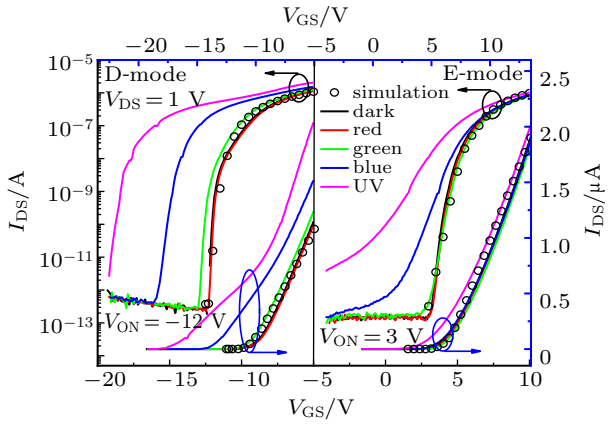

Fig. 2. Transfer curves of two kinds of a-IGZO TFTs by simulation, and measured in dark state and under different wavelength illumination under $V_{DS} = 1$ V in logarithmic scale (left, bottom axis) and linear scale (right, up axis).

Transfer curves of the two TFTs in the dark are simulated by Silvaco and fitted to the experimental data by adjusting the density of states (DOS) distribution within the band-gap. First, the transfer curve of the E-mode TFT is fitted and the fitting parameters are listed in the upper half of Table 1. g_{TA}(E) and g_{TD}(E) respectively represent the exponential distributions of acceptor-like and donor-like tail states, while $g_{GD}(E)$ is the Gaussian distribution of deep donor-like states related to neutral V_O.[8,9,21] Then, one continues to simulate the D-mode TFT characteristic by using the same g_{TA}(E) and g_{TD}(E), while adjusting g_{GD}(E) parameters and introducing shallow donor-like states g_{OV}(E)[21] near the conduction band edge (E_C). As shown in Fig. 2, the transfer curves of both kinds of TFTs in both linear and logarithmic scales are well fitted.

Comparing DOS parameters of the two TFTs, one finds that the neutral V_O density g_{GD}(E) of the D-mode TFT is 50 times higher than that of the E-mode TFT, and its energy levels distribution in the band-gap is 0.3 eV higher. Thus it is reasonable that the D-mode TFT is more photosensitive and

is also responsive to the green light. In addition, the introduced shallow donor states $g_{OV}(E)$ in the D-mode TFT, part of which above the Fermi-level (E_F) will ionize into V_O^{2+} and electrons, bring the large negative shift of V_{ON} relative to the E-mode TFT. Using the listed parameters of $g_{GD}(E)$ and $g_{OV}(E)$, the density of neutral V_O in E-/D-mode TFTs is calculated as 1.77×10^{16} cm^{-3}/8.85×10^{17} cm^{-3}, and the density of shallow V_O donors in D-mode TFTs is 3.94×10^{17} cm^{-3}.

Table 1. Fitting parameters of the two a-IGZO TFTs.

Parameters	Value	Description
E-mode a-IGZO TFTs		
N_C/cm^{-3}	2.0×10^{19}	effective DOS in CBM
N_V/cm^{-3}	5×10^{18}	effective DOS in VBM
E_g/eV	3.2	band-gap
Tail states acceptor-like DOS	$g_{TA}(E)=N_{TA}\exp[(E-E_C)/W_{TA}]$	
N_{TA}/eV^{-1}·cm^{-3}	1.4×10^{18}	density of tail states at $E=E_C$
W_{TA}/eV	0.36	conduction-band-tail slope
Tail states donor-like DOS	$g_{TD}(E)=N_{TD}\exp[(E_V-E)/W_{TD}]$	
N_{TD}/eV^{-1}·cm^{-3}	4.5×10^{19}	density of tail states at $E=E_V$
W_{TD}/eV	0.1	Valence-band-tail slope
Deep donor-like DOS	$g_{GD}(E)=N_{GD}\exp\{-[(E-E_{GD})/W_{GD}]^2\}$	
N_{GD}/eV^{-1}·cm^{-3}	1×10^{17}	density of donor-like at $E=E_V$
E_{GD}/eV	1	mean energy of donor-like
W_{GD}/eV	0.1	standard deviation of donor-like
D-mode a-IGZO TFTs		
Deep donor-like DOS	$g_{GD}(E)=N_{GD}\exp\{-[(E-E_{GD})/W_{GD}]^2\}$	
N_{GD}/eV^{-1}·cm^{-3}	5×10^{18}	density of donor-like at $E=E_V$
E_{GD}/eV	1.3	mean energy of donor-like
W_{GD}/eV	0.1	standard deviation of donor-like
Shallow donor-like DOS	$g_{OV}(E)=N_{OV}\exp\{-[(E-E_{OV})/W_{OV}]^2\}$	
N_{OV}/eV^{-1}·cm^{-3}	1×10^{18}	peak of OV states
E_{OV}/eV	2.9	mean energy of OV states
W_{OV}/eV	0.23	standard deviation of OV states

3.2. PPC effect in E-mode a-IGZO TFTs

Figures 3(a) and 3(b) are the time dependent photo-induced current ΔI (difference between I_D under light and dark) of an E-mode a-IGZO TFT for different light-intensities in the photo-excitation and recovery stages, respectively. ΔI of the recovery stage in Fig. 3(b) is normalized by its initial maximum value I_0 at the beginning of recovery. It is seen from Fig. 3(a) that increase of photocurrent in the photo-excitation stage tends to saturate with the illumination time, and the photo-response increases with increasing the light-intensity. In Fig. 3(b) the recovery of the photocurrent accelerates with the increasing light-intensity, which is consistent with the observations of most previous works.[7,11,12,14,15]

Time dependence of photocurrent rise and decay can be generally described by the stretch-exponential model.[22] Photocurrent rise follows

$$\Delta I(t)=I_S\{1-\exp[-(t/\tau_{ex})^{\beta_{ex}}]\}, \quad (1)$$

where I_S is the saturation value, τ_{ex} the photo-excitation time constant, and β_{ex} the stretch-exponent of photo-excitation. The PPC recovery follows

$$\Delta I(t)=I_0\{\exp[-(t/\tau_{re})^{\beta_{re}}]\}, \quad (2)$$

where I_0 is the initial value, τ_{re} the recovery time constant, and β_{re} the stretch-exponent of recovery. β is the ratio of thermal energy kT to a characteristic energy kT_0 of the trap distribution associated with the photo-excitation or recovery,

$$\beta=kT/kT_0=T/T_0. \quad (3)$$

In Fig. 3, one sees that the time evolution of ΔI in the photo-excitation and recovery stages for all light-intensities is well fitted by the stretch-exponential model.

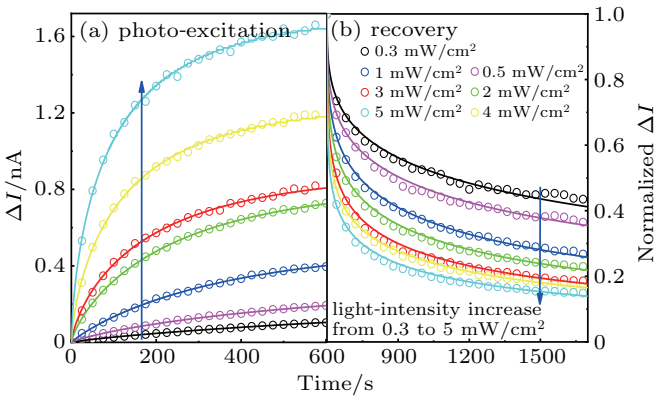

Fig. 3. The time dependent photo-induced current ΔI (difference between I_D under light and dark) are fitted with stretch-exponential model of an E-mode a-IGZO TFT for different light-intensities respectively in the (a) photo-excitation and (b) recovery stages. Hollow circles are experimental data, and solid lines are fitting curves.

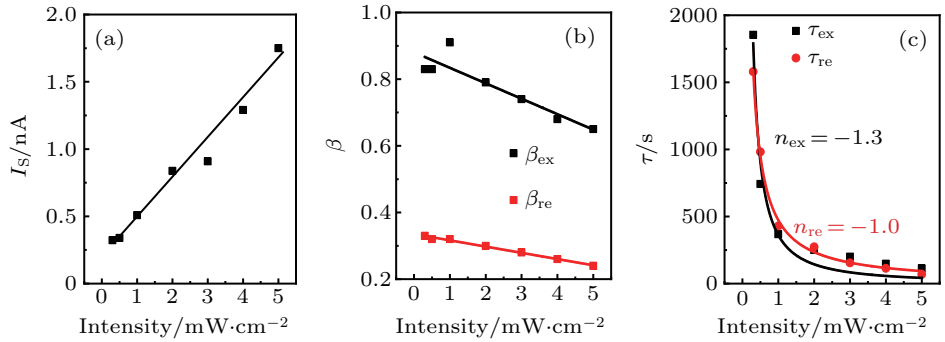

Fig. 4. Light-intensity dependence of (a) I_S; (b) β_{ex}, β_{re}; and (c) τ_{ex}, τ_{re}.

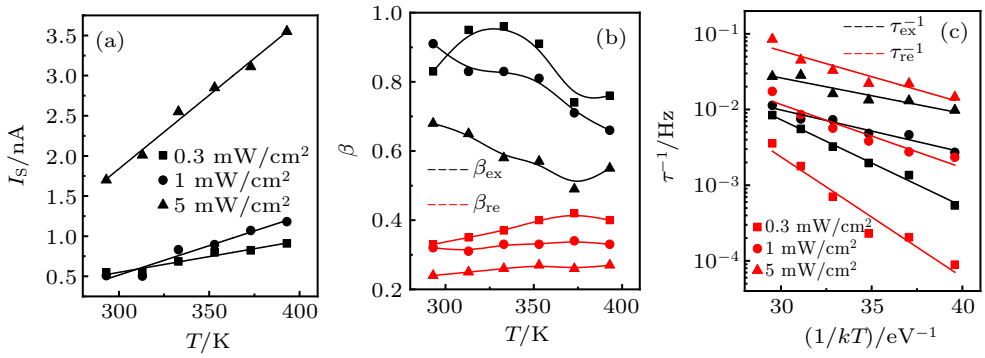

Fig. 5. The T dependence of (a) I_S; (b) β_{ex}, β_{re}; and (c) τ_{ex} τ_{re} under three light-intensities of 0.3 mW/cm^2, 1 mW/cm^2, and 5 mW/cm^2.

By fitting $\Delta I(t)$ to the stretch-exponential model, the characteristic parameters I_S, β_{ex}, and τ_{ex} for the photo-excitation and β_{re} and τ_{re} for the PPC recovery are readily extracted. Figure 4 shows their dependence on the light-intensity. Obviously in Fig. 4(a), I_S linearly increases with the light-intensity. In Fig. 4(b), both β_{ex} and β_{re} linearly decrease with the light-intensity. According to Eq. (3), decrease in β reflects the increase of the characteristic energy kT_0 of the involved traps in the photo-excitation or recovery. β_{ex} is much larger than β_{re}, indicating that distribution of the traps involved in the recovery is wider than that in the photo-excitation. In Fig. 4(c), one sees that both τ_{ex} and τ_{re} inversely decrease with the light-intensity with power exponents (n_{ex} and n_{re}) of their dependencies close to -1. Besides, τ_{ex} and τ_{re} for the same light-intensity are relatively close.

Then, photo-excitation and PPC recovery under selected light-intensities of 0.3 mW/cm^2, 1 mW/cm^2, and 5 mW/cm^2 are studied at six different temperatures from 293 K to 393 K. Figures 5(a)–5(d) show the T-dependencies of I_S, β_{ex}, and τ_{ex} for the photo-excitation, as well as of β_{re} and τ_{re} for the PPC recovery, for all three light-intensities. From Fig. 5(a), one sees that I_S linearly increases with T. In Fig. 5(b), β_{ex} decreases with T while β_{re} slightly increases with T. According to Eq. (3), it can be inferred that the characteristic energy kT_0 of traps distribution involved in the photo-excitation must strongly increase with T ($n > 1$), while kT_0 for traps in the recovery increases with T ($n = 0.23$–0.79).

From Fig. 5(c), one sees that both τ_{ex} and τ_{re} decrease with T, and they actually excellently follow the Arrhenius relationship

$$\tau^{-1} = \tau_0^{-1}\exp(-E_a/kT), \tag{4}$$

where E_a is the activation energy. It means that both the photo-excitation and PPC recovery are thermally activated processes. At higher temperatures, both photo-excitation process which induces metastable V_O^{2+} defects and free electrons, and the opposite recombination process of V_O^{2+} and free electrons in the dark would become easier. Thus the characteristic time τ_{ex} and τ_{re} become shorter. In Table 2, the extracted activation energies E_{a_ex} and E_{a_re} listed are for three light-intensities. One sees that both E_as become lower for higher light-intensities.

In previous works on PPC effect, the dependence of the PPC recovery activation energy on light-intensity was studied in Ref. [12], the activation energy for the photo-excitation was rarely observed. In Ref. [23], an E_a as high as ~ 0.5 eV for photoconductivity of a-IGZO films extracted in a narrow T range from room temperature to 60 °C was reported. It was attributed to the formation energy of photo-induced defects. In this study, much more solid data support that photo-induced V_O ionization and formation of metastable V_O^{2+} defects through lattice relaxation of adjacent metal cations are not a spontaneous process. Instead, microscopically overcoming a potential barrier must be involved and it is thermally activated. Furthermore, it is found that E_{a_ex} lowers under higher light-intensity. Plausibly, more defects are excited simultaneously and their collective relaxation may have some

synergistic mechanism. It could lower the potential barrier encountered by individual relaxation of fewer defects under lower light-intensity.

Table 2. Comparison of E_{a_ex} and E_{a_re} under three light-intensities.

Light-intensity	E_{a_ex}/eV	E_{a_re}/eV
0.3 mW/cm^2	0.25	0.22
1 mW/cm^2	0.13	0.19
5 mW/cm^2	0.11	0.15

3.3. PPC effect in D-mode a-IGZO TFTs

Figures 6(a) and 6(b) respectively show $\Delta I(t)$ of a D-mode a-IGZO TFT in the photo-excitation and PPC recovery stages, under different light-intensities, where ΔI in the recovery stage is also normalized. All data are well fitted with the stretch-exponential model. In Fig. 6, the photocurrents in both stages orderly change with the light-intensity. When the light-intensity is low, such as 0.01 mW/cm^2 or 0.05 mW/cm^2, photo-excited $\Delta I(t)$ rises within 600 s and is far from saturation. In contrary, the rise of $\Delta I(t)$ accelerates with time. In such conditions, the photo-excitation is insufficient, correspondingly PPC recovers quickly. While the light-intensity increases to 0.2 mW/cm^2 or above, the rise of $\Delta I(t)$ slows down with time and tends to saturate. Now the photo-excitation is sufficient, correspondingly the PPC recovery is much slower. Generally speaking, photocurrent under a higher light-intensity tends to saturate more quickly and its PPC recovery is much slower. However, the longest recovery time appears at a medium light intensity of 0.5 mW/cm^2. Such complicated light dependence is obviously different from that of E-mode TFTs.

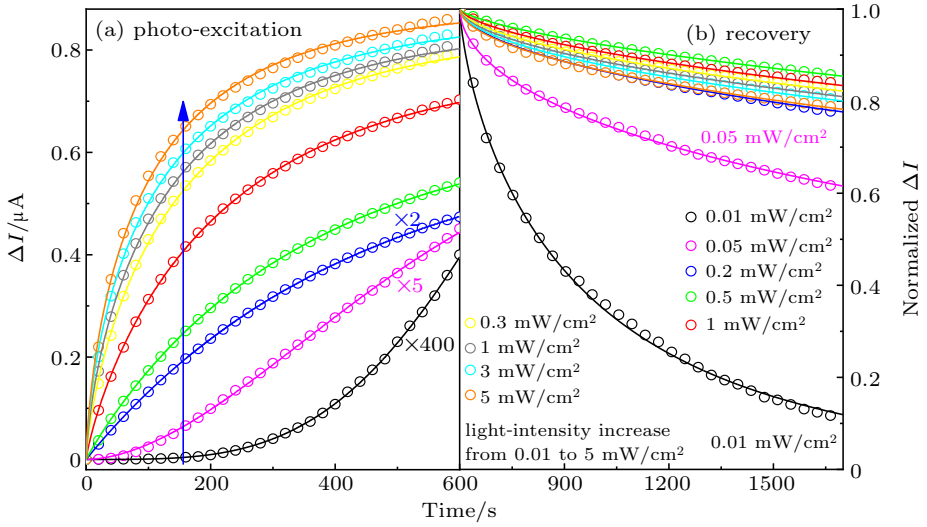

Fig. 6. The time dependent photo-induced current ΔI are fitted with the stretch-exponential model of a D-mode a-IGZO TFT for different light-intensities respectively in the (a) photo-excitation and (b) recovery stages. Hollow circles are experimental data, and solid lines are fitting curves.

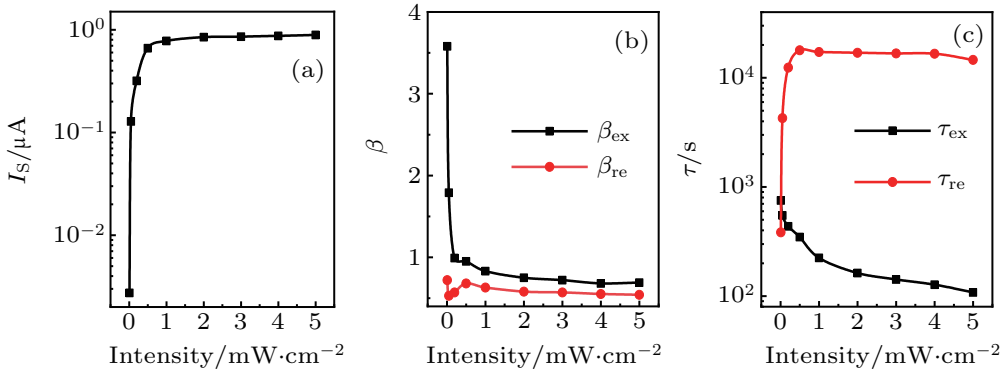

Fig. 7. Light-intensity dependence of (a) I_S; (b) β_{ex}, β_{re}; and (c) τ_{ex}, τ_{re}.

Figure 7 shows the light-intensity dependence of the photo-excitation parameters I_S, β_{ex}, and τ_{ex}, as well as of the PPC recovery parameters β_{re} and τ_{re}, which are extracted from the stretch-exponential model. Apparently, such dependence can be divided into two regions with different light-intensity dependencies: low (0.01–0.2 mW/cm^2) and high light-intensity ($>$ 0.2 mW/cm^2). As shown in Fig. 7(a), I_S rises steeply with the light-intensity in the low light-intensity region; while it only slightly increases with the light-intensity in the high light-intensity region. As shown in Fig. 7(b), in the low light-intensity region, $\beta_{ex} > 1$ and it sharply decreases with increasing light-intensity; while in the high light-

intensity region, both β_{ex} and β_{re} ($\beta_{ex} > \beta_{re}$) decrease slowly with increasing light-intensity, similar to those of E-mode TFTs in Fig. 4(c). As shown in Fig. 7(c), in the low light-intensity region, τ_{re} steeply rises with the light-intensity; while in the high light-intensity region, it remains almost stable and only slightly decreases with increasing light-intensity. For τ_{ex}, it simply decreases with increasing light-intensity, without showing a two-region dependency. In order to understand such complicated light dependency, we propose that a threshold dose of light-exposure is required to form photo-induced metastable V_O^{2+} defects in the a-IGZO channel. Under low light-intensity illumination, photo-excitation in 600 s is not enough to fully induce lattice relaxation of the adjacent metal cations, and to form a high PPC barrier. Correspondingly, the PPC recovery time is very short. By increasing the light-intensity, photo-excitation in 600 s becomes sufficient, then the metastable V_O^{2+} defects can be fully developed, leading to a sharp increase of the PPC recovery time.

Hence we replot the light dependency of the photo-excitation and PPC recovery parameters against the light-exposure in Fig. 8. The light-intensity ranges from 0.01 mW/cm^2 to 5 mW/cm^2, and the exposure time is 120 s, 300 s, and 600 s. Indeed, dependencies of I_S, β_{ex}, β_{re}, and τ_{re} have different behaviors, depending on its light-exposure lower or higher than a threshold dose of $\sim$ 150 mJ/cm^2. As shown in Fig. 8(a), I_S steadily increases with the light-exposure ($n = 1.1$) in the low light-exposure region, while it increases very slowly ($n = 0.16$) in the high light-exposure region. As shown in Fig. 8(b), in the low light-exposure region, both β_{ex} and β_{re} decrease with light-exposure ($n = -0.25$ and -0.12); while in the high light-exposure region, decrease of β_{ex} becomes much slower ($n = -0.11$), and β_{re} remains almost unchanged. As shown in Fig. 8(c), in the low light-exposure region, τ_{re} strongly increases with light-exposure ($n = 1.7$); while in the high light-exposure region it remains stable and has only a slight decrease with increasing light-exposure. In contrast, τ_{ex} simply decreases with increasing light-exposure in the whole range, and its power exponent $n = -0.28$ is obviously smaller than that of the E-mode TFTs in Fig. 4(c). Based on the observations, one can determine that there is a threshold dose of light-exposure $\sim$ 150 mJ/cm^2, above which significant PPC effect occurs, and below which photo-induced metastable defects are under development.

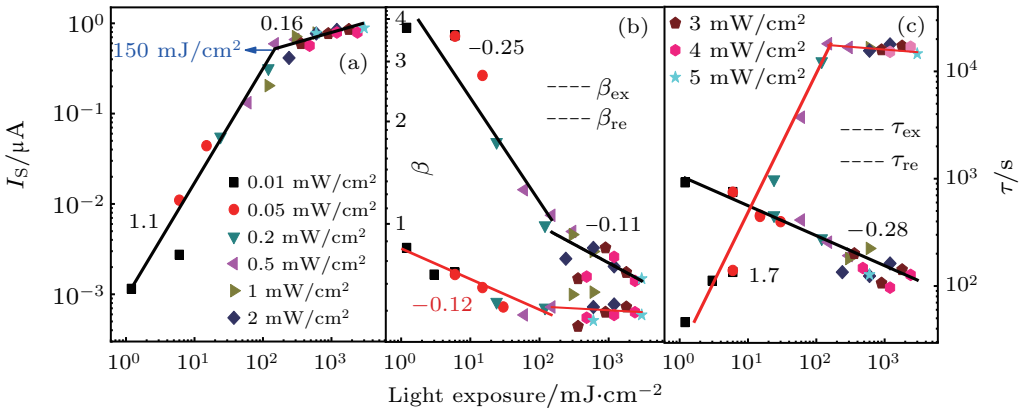

Fig. 8. Light-exposure dependence of (a) I_S; (b) β_{ex}, β_{re}; and (c) τ_{ex}, τ_{re} in double logarithmic scales.

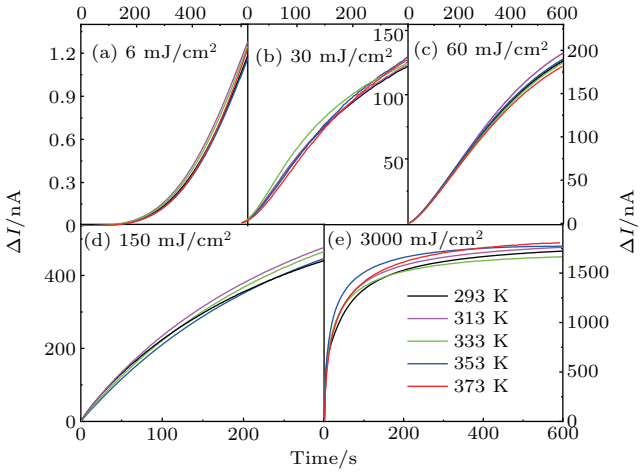

Fig. 9. The change of ΔI with illumination time in photo-excitation stage at five different temperatures for light-exposures of (a) 6 mJ/cm^2, (b) 30 mJ/cm^2, (c) 60 mJ/cm^2, (d) 150 mJ/cm^2, and (e) 3000 mJ/cm^2.

To check the hypothesis, photo-excitation and PPC recovery under three light-exposures below the threshold (6 mJ/cm^2, 30 mJ/cm^2, and 60 mJ/cm^2) and two light-exposures above the threshold (150 mJ/cm^2 and 3000 mJ/cm^2) are investigated at different Ts from 293 K to 373 K. Figure 9 shows the photo-excited $\Delta I(t)$ curves under different Ts for all five light-exposures. As shown in Figs. 9(a)–9(c) for low light-exposures below the threshold, the $\Delta I(t)$ curves are featured by their unsaturation. While for high light-exposures above the threshold in Figs. 9(d)–9(e), the $\Delta I(t)$ curves obviously tend to saturation. However, regardless of light-exposures, all $\Delta I(t)$ curves are little affected by Ts. It means that in D-mode TFTs, photo-excitation is not thermal activated but a spontaneous process. It is distinctly different from that in E-mode TFTs in Fig. 5(c).

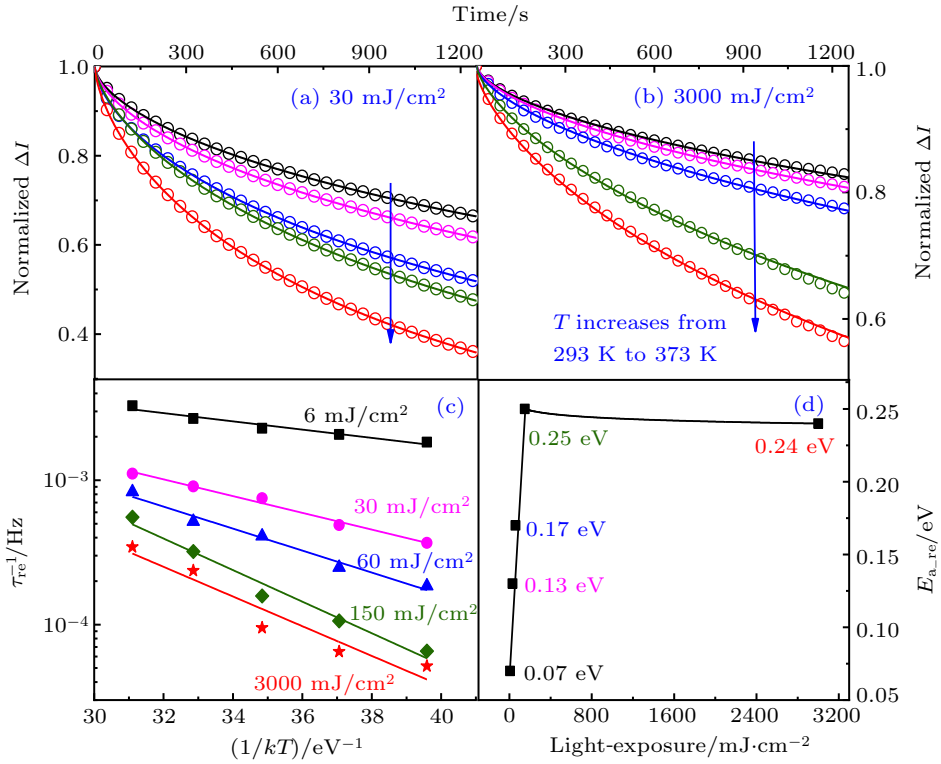

Fig. 10. The time dependent normalized current ΔI are fitted with stretch-exponential model for different temperatures in the recovery stage at (a) 30 mJ/cm^2 and (b) 3000 mJ/cm^2; (c) $1/kT$ dependence of τ_{re}^{-1}; (d) light-exposure dependence of E_{a_re} extracted from (c).

PPC recovery $\Delta I(t)$ curves at different Ts are shown in Figs. 10(a) and 10(b) for two representative light-exposures of 30 mJ/cm^2 and 3000 mJ/cm^2 (below and above the threshold). Clearly, the PPC recovery is faster at higher Ts, regardless of its light-exposures. Figure 10(c) shows $1/T$ dependence of τ_{re}^{-1} for all five light-exposures, which excellently follows the Arrhenius relationship. Hence activation energies E_{a_re} are extracted and plotted against light-exposure in Fig. 10(d). Impressively, one sees that in the region below the threshold, E_{a_re} rapidly increases with light-exposure from 0.07 eV to 0.25 eV; while in the region above the threshold, E_{a_re} remains basically unchanged, slowly decreasing from 0.25 eV to 0.24 eV. It specifically describes the formation of photo-induced metastable defects. Below the threshold dose, photo-excitation is insufficient to form fully developed metastable defects. At this stage, the PPC barrier is low and it grows with light-exposure. However, increasing the light-exposure above the threshold, the photo-induced defects can now be fully developed. The PPC barrier is built and remains stable, which does not grow with light-exposure anymore. On the contrary, the electron density grows due to V_O ionization under continuously increased light-exposure, partially shielding the PPC barrier. The effective barrier is slightly reduced.

4. A unified model of photo-induced defects

Table 3 summarizes the PPC light-dependency of E-mode and D-mode a-IGZO TFTs. E-mode TFTs have fewer V_O defects and lower photo-response. Both photo-excitation and recovery are thermally activated, and the related E_as decrease with increasing the light-intensity. D-mode TFTs have much more V_O defects, and higher photo-response. The photo-excitation is independent of T, while the PPC recovery is thermally activated. Its light-dependency has two regions. In the sub-threshold region, photocurrent I_S increases linearly with the light-exposure, β_{ex} decreases and the PPC barrier sharply increases, and τ_{re} also sharply increases. However, in the above-threshold region, I_S increases slowly, β_{ex} decreases slowly, the PPC barrier keeps stable, and τ_{re} decreases slightly.

Table 3. Comparison of PPC light dependency of E-mode and D-mode a-IGZO TFTs. The values represent the power exponent n in the power exponent relationship between the relevant parameters and light-intensity or exposure, and the arrows (↑ ↓) represent the increase or decrease with the increase of the light-intensity or exposure.

Samples		Photo-excitation				PPC recovery		
		I_S	β_{ex}	τ_{ex}	E_{a_ex}	β_{re}	τ_{re}	E_{a_re}
E-mode TFTs		1	↓	−1	↓	↓	−1	↓
D-mode TFTs	$< D_T$	1.1	−0.25	−0.28	–	−0.12	1.7	↑
	$> D_T$	0.16	−0.11	−0.28	–	–	slightly ↓	slightly ↓

Considering the photo-excitation and PPC recovery characteristics of the two kinds of TFTs, we propose a unified model of photo-induced metastable defects of a-IGZO TFTs, which is based on two key factors: density of V_O defects in the channel and light illumination. In E-mode TFTs there are fewer V_O defects. Formation of the photo-induced metastable defects is thermally activated, and E_a continuously decreases with light-intensity. While in D-mode TFTs there are a large number of V_O defects, the photo-induced defect formation is spontaneous. Nevertheless, it is first found that a threshold dose of light-exposure is required to form fully developed photo-induced metastable defects. In sub-threshold light-exposure region, insufficient photo-excitation can only form a low PPC barrier. Increasing the light-exposure above the threshold, the lattice relaxation of metal cations adjacent to V_O^{2+} can be fully developed and the barrier increases to ~ 0.25 eV, which remains stable for larger light-exposures. It is noticed that only a previous PPC study on Se–Ge–In material[13] ever proposed that photo-induced defects structural change increases with light-intensity. While this study is the first work providing strong evidence on formation of the metastable defects depending on light-exposure.

5. Conclusions

In this paper, we have systematically studied the light-intensity dependence of PPC of E-/D-mode a-IGZO TFTs. Density of V_O defects of E-mode TFTs is relatively small, in which formation of the photo-induced metastable defects is thermally activated, and the activation energy (E_a) decreases continuously with increasing light-intensity. Density of V_O defects of D-mode TFTs is much larger, in which the formation of photo-induced metastable defects is found to be spontaneous instead of thermally activated. Furthermore, for the first time it is found that a threshold dose of light-exposure is required to form fully developed photo-induced metastable defects. Based on the density of V_O defects in the channel and the condition of light illumination, a unified model of formation of photo-induced metastable defects in a-IGZO TFTs is proposed.

References

[1] Nomura K, Ohta H, Takagi A, Kamiya T, Hirano M and Hosono H 2004 *Nature* **432** 488
[2] Kamiya T, Nomura K and Hosono H 2009 *Display Technology, Journal of* **5** 273
[3] Lee M, Kim K T, Lee M, Parkb S K and Kim Y H 2018 *Thin Solid Films* **660** 749
[4] Jeon S, Ahn S E, Song I, Kim C J, Chung U I, Lee E, Yoo I, Nathan A, Lee S, Robertson J and Kim K 2012 *Nat. Mater.* **11** 301
[5] Tanabe T, Notomi M, Mitsugi S, Shinya A and Kuramochi E 2005 *Opt. Lett.* **30** 2575
[6] Liu M Y, Chen E and Chou S Y 1994 *Appl. Phys. Lett.* **65** 887
[7] Lu M P, Lu M Y and Chen L J 2014 *Adv. Funct. Mater.* **24** 2967
[8] Lany S and Zunger A 2005 *Phys. Rev. B* **72** 035215
[9] Janotti A and Van De Walle C G 2005 *Appl. Phys. Lett.* **87** 122102
[10] Kim J Y, Yu K M, Jeong S H, Yun E J and Bae B S 2014 *Can. J. Phys.* **92** 611
[11] Moore J C and Thompson C V 2013 *Sensors* **13** 9921
[12] Worasawat S, Tasaki K, Neo Y, Pecharapa W, Hatanaka Y and Mimura H 2019 *Jpn. J. Appl. Phys.* **58** 055505
[13] Singh S, Shukla R K and Kumar 2005 *Indian Journal of Engineering and Materials Sciences* **12** 461
[14] Polyakov A Y, Smirnov N B, Govorkov A V and Redwing J M 1998 *MRS Proceedings* **512** 537
[15] Sarkar N, Dhar S and Ghosh S 2003 *J. Phys.: Condens. Matter* **15** 7325
[16] Lee J M, Cho I T, Lee J H and Kwon H I 2009 *Jpn. J. Appl. Phys.* **48** 100202
[17] Wang M, Liang L, Luo H, Zhang S, Zhang H, Javaid, K and Cao H 2016 *IEEE Electron Dev. Lett.* **37** 422
[18] Lu L, Li J and Wong M 2015 *IEEE Trans. Electron Dev.* **62** 3703
[19] Feng Z, Lu L, Wong M and Kwok H S 2016 *Sid Symposium Digest of Technical Papers* **47** 1197
[20] Lany S and Zunger A 2010 *Phys. Rev. B* **81** 113201
[21] Kim Y, Kim S, Kim W, Bae M, Jeong H. K, Kong D, Choi S, Kim D. M and Kim D H 2012 *IEEE Trans. Electron Dev.* **59** 2699
[22] Luo J, Adler A U, Mason T O, Buchholz D B, Chang R P H and Grayson M 2013 *J. Appl. Phys.* **113** 153709
[23] Lee D H, Kawamura K I, Nomura K, Yanagi H, Kamiya T, Hirano M and Hosono H 2010 *Thin Solid Films* **518** 3000